XGEOSTARE: Extensible GEO Space-based Telescopes for Actionable Refinement of Ephemerides

Nathan Golovich, Robert Armstrong, Alex Geringer-Sameth, and Benjamin Bahney
Lawrence Livermore National Laboratory

Gary Li
Impulse Space Inc.

ABSTRACT

We present a novel approach to space situational awareness (SSA) using an extensible network of low-cost, commercial off-the-shelf (COTS) small satellites and payloads. This architecture addresses the growing challenge of tracking the increasing population of faint objects in Earth orbit, especially in geostationary orbit (GEO) and cislunar space. Through simulation, we quantify trade-offs between aperture size, field of view, satellite count, and target faintness, demonstrating that a distributed COTS network can achieve effective coverage and sensitivity. The system's modular-ity enables straightforward integration of additional satellites to improve performance and extend coverage to diverse orbital regions. By leveraging commercial components rather than bespoke systems, the approach remains scalable and cost controlled. This work highlights a practical pathway to balance the need for high sensitivity with the constraints of small spacecraft, supporting sustainable satellite operations, debris mitigation, and long-term space safety.

1. INTRODUCTION

The rapid growth of operational satellites and debris in Earth orbit and new activity in cislunar space have created demand for scalable situational awareness. Traditional government-developed systems are effective but costly and not easily extensible. This paper introduces a novel approach based on commercial off-the-shelf (COTS) small satellites and payloads. We analyze the coverage and sensitivity achievable for two key regions: (1) geostationary orbit (GEO) and (2) cislunar orbits, including Lagrange point halo and tadpole orbits and distant retrograde orbits (DROs). We compare these metrics across payload apertures and constellation sizes.

2. BACKGROUND AND RELATED WORK

Existing GEO surveillance relies heavily on ground-based optical sensors and a limited number of costly dedicated satellites. These systems face constraints in weather, cost, and scalability. Cislunar space situational awareness (SSA) presents even greater challenges due to the vast volumes involved and the faintness of resident objects. Previous concepts emphasized bespoke, high-cost spacecraft that did not address data-rate challenges and are not easily scalable to the growing demand for SSA in the coming years. In contrast, COTS systems have the potential to reduce costs and expand rapidly. This study builds on prior analyses by explicitly quantifying trade-offs between sensitivity, coverage, and constellation size in both GEO and cislunar regimes while also considering data rates and the performance of edge computing platforms, which have rapidly improved in efficiency and computational throughput.

3. SYSTEM CONCEPT AND ASSUMPTIONS

We consider a constellation of small satellites equipped with modest apertures and commercial detectors. The payload design emphasizes wide field of view, moderate sensitivity, autonomous operation, inter-satellite communication, and onboard detection processing. Key parameters include aperture diameter, field of view, integration time, limiting magnitude, orbital placement, and constellation size. We assume realistic detector performance (quantum efficiency, dark current, read noise) and standard illumination conditions for GEO and cislunar regions (sunlight, Earthshine, and Moonshine). The architecture is designed to be extensible: additional satellites can be added incrementally to expand coverage. Our fiducial model is a GEO+1000 km ring of satellites spaced evenly in longitude (see Figure 1).

Copyright © 2025 Advanced Maui Optical and Space Surveillance Technologies Conference (AMOS) – www.amostech.com

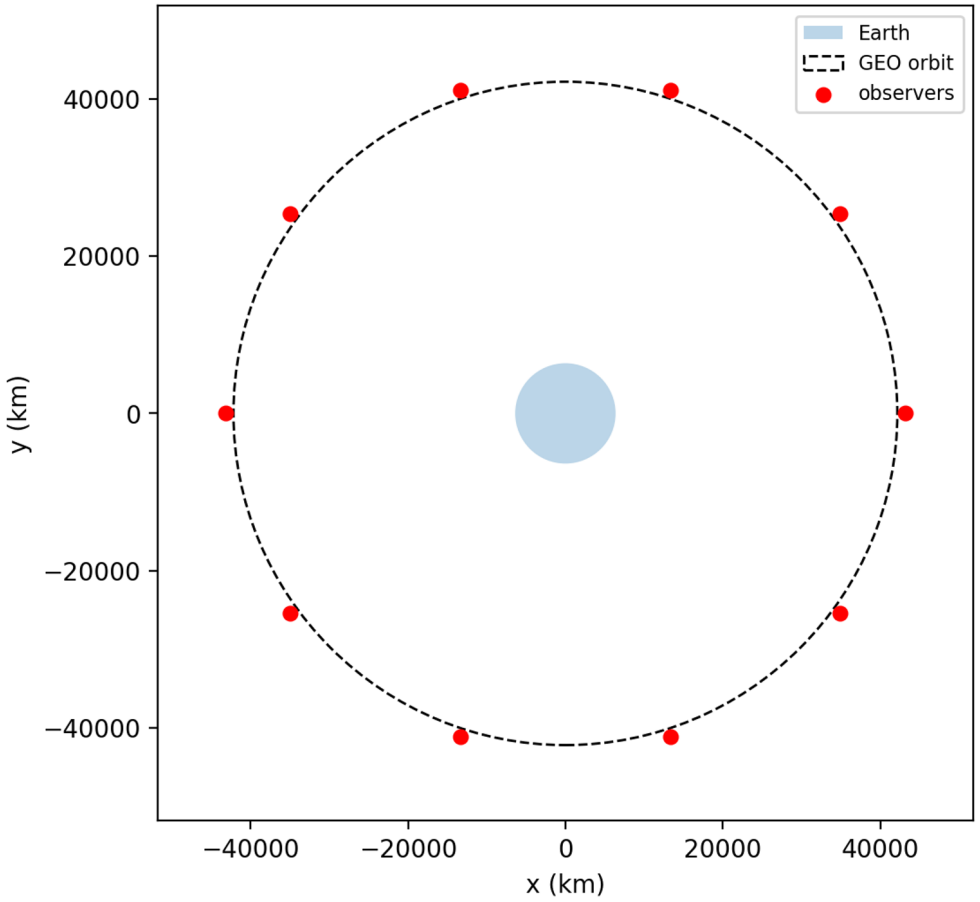

Fig. 1: Conceptual architecture of the COTS-based SSA constellation operating 1000 km above GEO (GEO+1000 km ring).

4. METHODOLOGY

4.1 Simulation setup

We developed a simulation framework to evaluate coverage and sensitivity for the two orbital regimes. Coverage is quantified in terms of detectability of targets, averaged over time, and geometric access to target regions given nominal solar, Earth, and lunar exclusion angles. Sensitivity is estimated using standard photometric models that account for aperture size, integration time, zodiacal light [10, 8], and detector noise. Proper baffling is assumed to suppress correlated noise from internal reflections. Target brightness follows a Lambertian sphere reflectance model accounting for flux from the Sun, Earth, and Moon. Trade-offs are explored by varying aperture, field of view, number of satellites, and target faintness.

For cislunar cases, our workflow ingests files from the JPL three-body periodic orbits API [1] that contain circularly restricted three-body problem (CR3BP) normalized initial conditions for selected Earth–Moon orbits (L1 and L2 halo, L4 and L5 short-period tadpole, and DRO). Each seed is integrated with a rotating-frame fourth-order Runge-Kutta (RK4) propagator over two periods to generate state tracks. Figure 2 shows the orbits selected in our analysis.

[1] https://ssd.jpl.nasa.gov/tools/periodic_orbits.html#/intro

Copyright © 2025 Advanced Maui Optical and Space Surveillance Technologies Conference (AMOS) – www.amostech.com

Apparent magnitude model

We estimate apparent magnitude by summing the irradiance on the target from direct sunlight, Earthshine, and Moonshine, then reradiating toward the observer with a Lambertian bidirectional model. The flux received by the observer is

$$F_{\text{obs}} \;=\; \frac{A_{\text{t}}\, p_{\text{t}}\, \Phi_{\text{t}}(\alpha_{\text{obs}})}{\pi \Delta^2} \Big[E_{\odot\to\text{t}} \;+\; E_{\text{Earth}\to\text{t}} \;+\; E_{\text{Moon}\to\text{t}} \Big], \tag{1}$$

where A_{t} is the target cross section, p_{t} the geometric albedo, $\Phi_{\text{t}}(\alpha_{\text{obs}})$ the target phase function toward the observer at the phase angle α_{obs}, and Δ the observer–target distance.

The irradiance terms at the target are

$$E_{\odot\to\text{t}} = \frac{F_{\odot}(1\,\text{AU})}{r_{\odot\text{t}}^2}, \tag{2}$$

$$E_{\text{Earth}\to\text{t}} = \frac{F_{\odot}(1\,\text{AU})}{r_{\odot\text{E}}^2}\, A_{g,\text{E}}\, \Phi_{\text{E}}(\alpha_{\odot\text{E}})\, \frac{R_{\text{E}}^2}{r_{\text{Et}}^2}, \tag{3}$$

$$E_{\text{Moon}\to\text{t}} = \frac{F_{\odot}(1\,\text{AU})}{r_{\odot\text{M}}^2}\, A_{g,\text{M}}\, \Phi_{\text{M}}(\alpha_{\odot\text{M}})\, \frac{R_{\text{M}}^2}{r_{\text{Mt}}^2}, \tag{4}$$

with $F_{\odot}(1\,\text{AU})$ the solar irradiance at 1 AU; $r_{\odot\text{t}}$ the Sun–target distance; $r_{\odot\text{E}}$ and $r_{\odot\text{M}}$ the Sun–Earth and Sun–Moon distances; $A_{g,\text{E}}$ and $A_{g,\text{M}}$ the geometric albedos of Earth and Moon; Φ_{E} and Φ_{M} their disk phase functions (normalized to 1 at full phase); R_{E} and R_{M} their radii; and r_{Et}, r_{Mt} the Earth–target and Moon–target distances.

The conversion to apparent magnitude in the chosen band is

$$m \;=\; -2.5 \log_{10}\!\left(\frac{F_{\text{obs}}}{F_0} \right), \tag{5}$$

where F_0 is the photometric zero point for that band. We assume V band and set the solar flux to the equivalent of $m_V = -26.74$ [14]. Our limiting magnitudes for different sensor configurations all assume the noise characteristics given in Table 1. The assumed payloads are variations of Lawrence Livermore National Laboratory's monolithic telescopes with Sony IMX unfiltered monochromatic cameras [12].

Table 1: Key parameters used in the simulation framework.

Parameter	Value / Range
Aperture diameter [cm]	8.5, 17.5, 25
Bandpass	V
Target magnitude (GEO)	$15 < m_V < 22$
Target magnitude (cislunar)	$m_V = 21$
Target radius (GEO) [cm]	10
Target radius (cislunar) [cm]	50
Target geometric albedo	0.20
Earth geometric albedo	0.30
Moon geometric albedo	0.12
Solar V magnitude	-26.74
Read noise [e^- pix^{-1}]	1.8
Dark current [e^- s^{-1} pix^{-1}]	0.81
Sky surface brightness [mag arcsec^{-2}]	22

4.2 Performance estimation

Each sensor–target pair is analyzed against discriminating cuts based on target brightness, solar elongation, Earth elongation, and lunar elongation. These cuts approximate operational constraints and define whether a given observation is geometrically and photometrically feasible.

Copyright © 2025 Advanced Maui Optical and Space Surveillance Technologies Conference (AMOS) – www.amostech.com

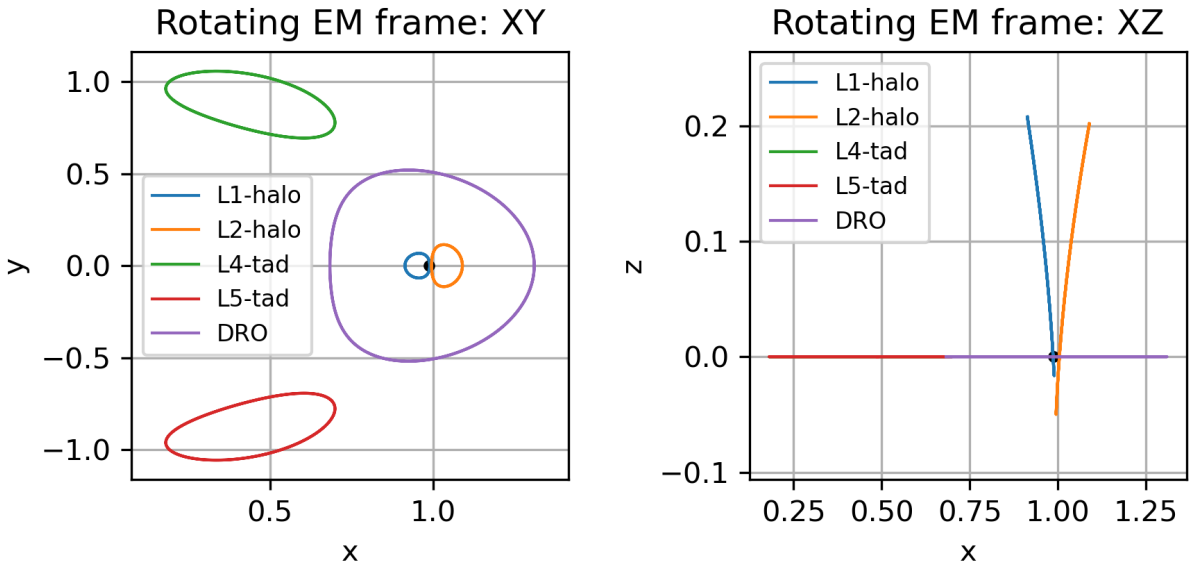

Fig. 2: Selected cislunar trajectories in the rotating Earth–Moon frame. The trajectories all come from the JPL periodic orbits catalog.

Target brightness is modeled using a simplified photometric equation that accounts for intrinsic magnitude, phase angle, and range to the observer, including Earthshine and Moonshine. A limiting magnitude threshold is applied based on aperture size, integration time, and detector characteristics. Solar elongation cuts remove geometries where the target lies too close to the Sun. Earth and lunar elongation thresholds avoid observations where stray light and background noise are prohibitive in near-limb geometries.

The simulation is run over a period of 10 years to pose a wide range of possible Earth–Moon–Sun geometries to the system. At each time step, potential observations are flagged valid if all cuts are passed. The resulting time series provides a basis for computing performance metrics. Performance is aggregated across all satellites in the network to quantify constellation-level effectiveness in GEO and cislunar regimes.

Specifically for cislunar estimation, Astropy ephemerides [1, 2, 3] build an Earth–Moon line triad per timestamp to map the nondimensional tracks to geocentric distance. Targets are sampled along each track, and observability is evaluated under Sun/Earth/Moon cuts. For cislunar analysis, we assume a more agressive lunar exclusion threshold to enable near Moon observations of targets in L1 halo, L2 halo, and DRO orbits.

Table 2: Representative performance cuts applied to each sensor–target pair.

Criterion	Threshold
Solar elongation	$\geq 45^\circ$
Earth limb elongation	$\geq 20^\circ$
Lunar elongation	$\geq 15^\circ$ (GEO), $\geq 5^\circ$ (cislunar)
Limiting magnitude (1 second exposure)[1]	15.8, 17.2, 18.0
Limiting magnitude (10 second exposure)[1]	17.8, 19.5, 20.2

[1] Limiting magnitudes are for 8.5, 17.5, and 25 cm aperture, respectively.

4.3 Binocular ranging

An added benefit of a constellation in the GEO vicinity is the ability to improve initial orbit determinations (IODs) via binocular ranging. When two or more sensors observe the same target nearly simultaneously, their angular measurements can be combined to form intersecting lines of sight. The intersection geometry provides a range estimate via

Copyright © 2025 Advanced Maui Optical and Space Surveillance Technologies Conference (AMOS) – www.amostech.com

parallax, reducing reliance on angular-only methods [13, 6, 11], which suffer large uncertainties, particularly cislunar objects where the distance is not known. Angles only methods typically require a strong prior on the range and radial velocity to estimate position and velocity of the target. This is unnecessary when parallax in included in the motion model.

In our analysis, we assume time-synchronized observations between satellite pairs separated by 180° in GEO longitude. The baseline separation provides sufficient parallax to resolve range with meaningful accuracy, even when measurement errors are on the order of arcseconds. By fusing binocular range estimates with conventional angles-only tracking, the covariance of the target state vector contracts significantly, leading to faster convergence in orbit determination.

Effectiveness is quantified through Monte Carlo simulations in which target orbits are reconstructed using angular-only and angular-plus-range measurements. We simulate detections of a cislunar target in an L1 halo orbit with a single sensor or two GEO sensors separated by 180°. Improvement is measured by estimating position and velocity from one hour of observations at 10-minute cadence. We assume 1″ centroid errors for all angular measurements. A Gaussian prior was imposed on the object's initial geocentric range (mean 326,400 km, σ = 40,000 km) to regularize the otherwise ill-posed single-station geometry. See Figure 3 for a schematic.

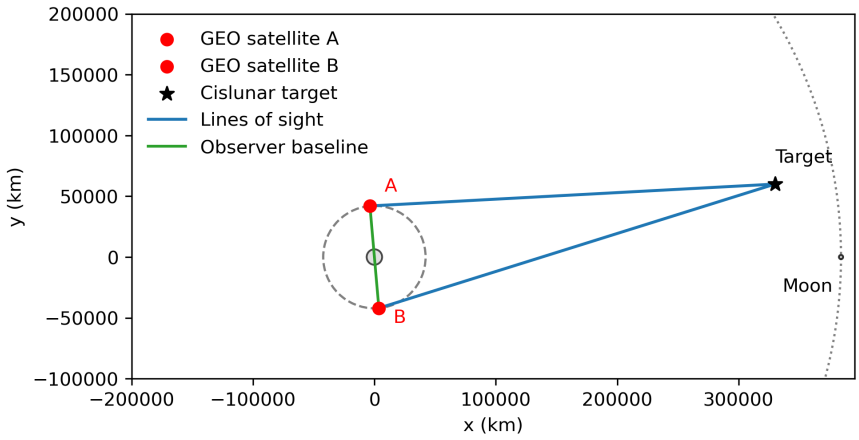

Fig. 3: Conceptual schematic of binocular ranging. Two GEO-region satellites observe the same target, and their lines of sight intersect to provide a direct range estimate.

5. RESULTS

5.1 GEO coverage

We varied constellation size for the fiducial configuration (Figure 1) and placed target populations in the GEO region. In each iteration, ten thousand targets were assigned a 10 cm radius and 20% albedo and placed randomly at GEO altitude with an inclination up to 30°. Initial Sun, Earth, and Moon positions were randomized 100 times across a year. Visibility of each target was computed using Table 2. Figure 4 shows the median result over 1000 bootstrap realizations of the Sun–Earth–Moon geometry spanning 10,000 days to capture angular deviations in the reflection model. Coverage improves with additional GEO observers and higher sensitivities (larger apertures). The vertical lines show representative apertures and sensitivities for 1–10 s exposures. Results suggest that a modest constellation of 25 cm aperture telescopes can cover GEO.

This result carries a caveat: the wide inclination range requires large sky coverage. Figure 5 shows a representative on-sky view for a sensor. Visible targets span thousands of square degrees. Most are along-track in GEO, but Earthward points appear spread. These should be left for adjacent observers. Figure 6 shows the projected view for one sensor in the XY plane.

Simulations show how constellation size and aperture drive limiting magnitudes and coverage. The challenge is spatial coverage: detectable GEO targets span 2000–10,000 deg^2 depending on Sun and Moon. Restricting inclination

Copyright © 2025 Advanced Maui Optical and Space Surveillance Technologies Conference (AMOS) – www.amostech.com

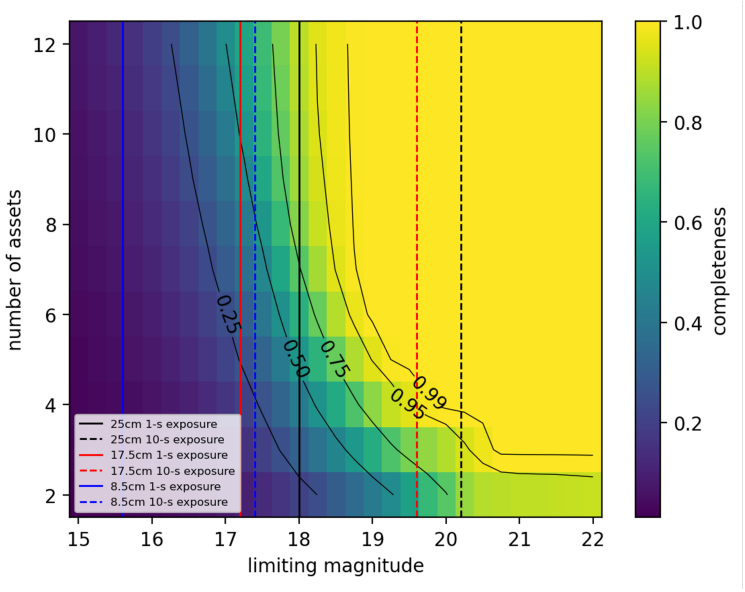

Fig. 4: Coverage completeness in GEO as a function of constellation size.

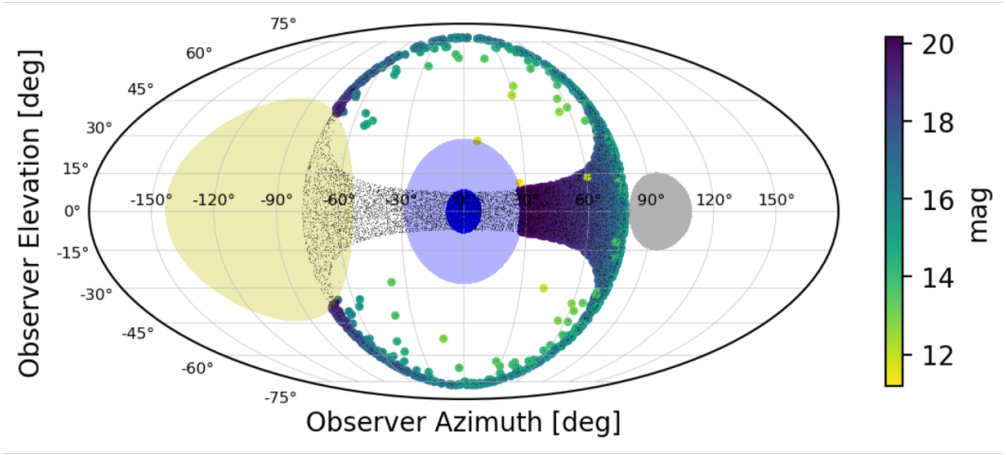

Fig. 5: Observer on-sky view for one constellation member. Colored points are brighter than the 25 cm, 10 s limiting magnitude of 20.2. Black points are fainter. The shaded regions are Earth (blue), Moon (gray), and Sun (yellow) exclusion zones. The spatial extent of the colored points is 4500 deg^2. Other sensors require 2000–10,000 deg^2.

to 15° reduces coverage per sensor to 1000–7000 deg^2. Increasing sensor altitude compresses the belt into a smaller region but increases target distance, requiring more satellites. At GEO+10,000 km, angular coverage decreases but constellation size must grow.

5.2 Cislunar coverage

For cislunar space, detection is harder due to distance and faintness. We examined the GEO+1000 km ring constellation's capabilities for L1/L2 halos, L4/L5 tadpoles, and DROs.

Additional GEO sensors add little to cislunar coverage, since distance is roughly constant and exclusion zones average out. Performance variability depends on orbit fraction lost to exclusion zones and distance differences.

Results show that roughly half the time, cislunar coverage is possible with 25 cm visible telescopes in GEO. Longer exposures improve sensitivity but not fully: phase-angle variations yield times when targets are too faint regardless of occlusion. About one quarter of observations were lost to occlusions, primarily Sun and Moon. Recovery may require

Copyright © 2025 Advanced Maui Optical and Space Surveillance Technologies Conference (AMOS) – www.amostech.com

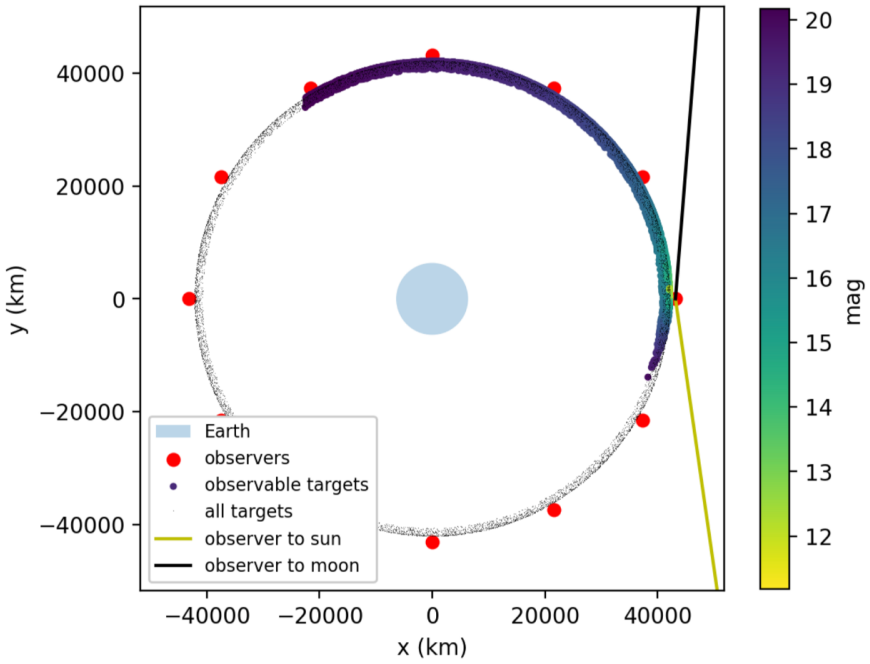

Fig. 6: Projected view of the GEO vicinity and visible objects from one observer in the GEO+1000 km ring. Colored and black points correspond to those in Figure 5. Redundancy is evident with 12 observers in this configuration.

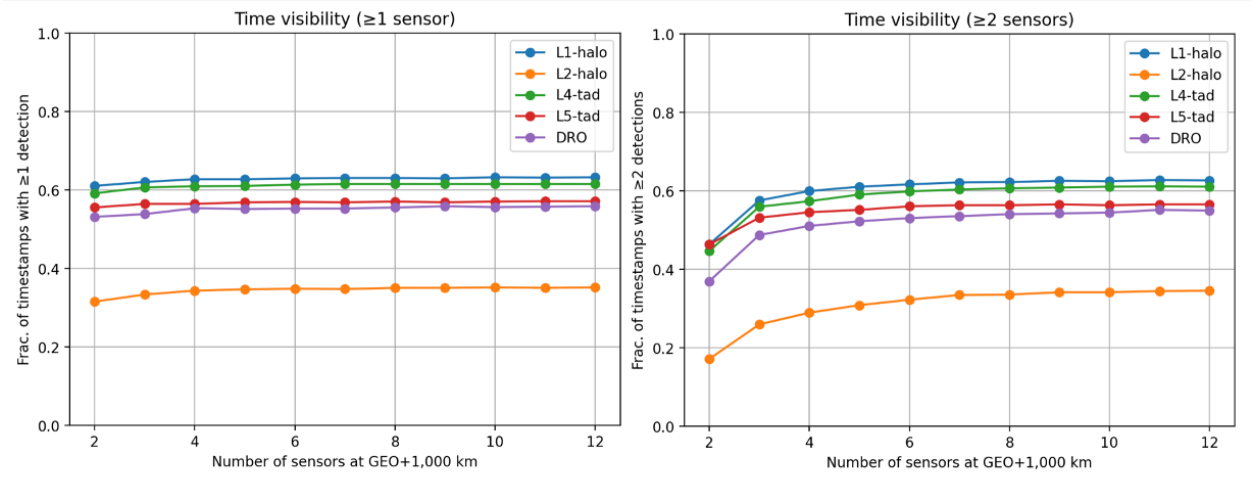

Fig. 7: Coverage fraction of selected cislunar orbits over 1 year as a function of constellation size. Left: fraction of the year observable by at least one sensor. Right: same for at least two sensors.

shrinking exclusion zones or adding sensors in diverse orbits within cislunar space.

5.3 Binocular ranging cislunar targets

We quantified dual-sensor benefits for a cislunar target in an L1 halo. Two GEO observers phased 180° apart observed a target oriented perpendicular to their baseline. A one-hour arc with 10-minute cadence was simulated. Motion was modeled as constant velocity in the Earth-centered inertial frame. Each observation was a line-of-sight vector with Gaussian centroid error of $1''$ RMS. A Gaussian prior was applied on range (mean 326,400 km, $\sigma = 40{,}000$ km).

Monte Carlo trials generated noisy data, solved with nonlinear least squares. Each trial was solved twice: once with a single observer plus range prior, and once with both observers. Covariance matrices were approximated from

Copyright © 2025 Advanced Maui Optical and Space Surveillance Technologies Conference (AMOS) – www.amostech.com

Jacobians. With 1″ measurements over one hour, single-sensor fits yielded ∼8,600 km position and ∼1.3 km/s velocity errors, while dual-sensor fits reduced errors to ∼6.5 km and ∼0.003 km/s.

Our assumption of 180° longitude separation between observers is the maximum. Here, we analyze the benefit of a range of baselines between observers. For each chosen baseline GEO, Monte Carlo trials are repeated to sample measurement noise, and the ratio of single-sensor to dual-sensor root mean square errors in position and velocity is reported as an "improvement factor". By sweeping baselines from kilometers up to the maximum GEO chord length, the analysis produces curves of mean improvement factors with 1σ error bars, directly illustrating how increasing observer separation reduces state uncertainty in both position and velocity. The results are shown in Figure 8.

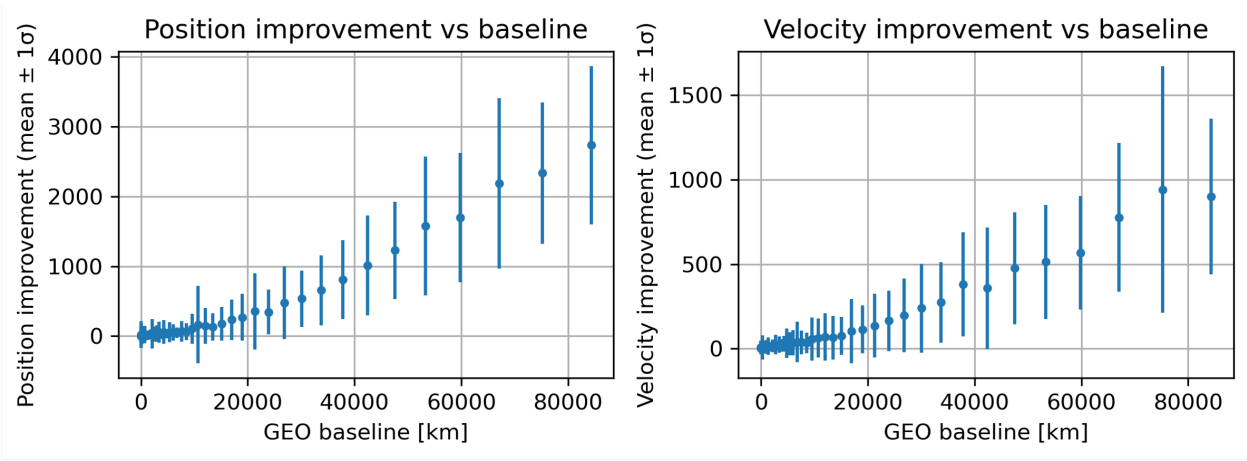

Fig. 8: IOD improvement factor for two satellites compared to a single satellite observation of an L1 halo object. Points show the mean of 10,000 Monte Carlo realization of the observation and error bars show the 1σ deviation in the improvement factor for the position (left) and velocity (right) error in the estimate.

6. DISCUSSION

The results of this study demonstrate that a constellation of small, commercially sourced satellites can provide meaningful contributions to space situational awareness (SSA) in both geostationary (GEO) and cislunar regimes. By quantifying coverage and sensitivity trade-offs, we show that modest-aperture telescopes in a GEO+1000 km ring can monitor large portions of the GEO belt, while also achieving partial coverage of representative cislunar trajectories. Furthermore, binocular ranging between paired observers provides dramatic improvement in orbit determination accuracy, reducing position and velocity uncertainties by orders of magnitude compared to single-station methods. These findings establish a baseline for how low-cost, extensible constellations may complement traditional, bespoke systems.

6.1 Implications for SSA Architectures

The key implication of our work is that performance scaling can be achieved with incremental satellite additions rather than large monolithic investments. For GEO, we find that a constellation of 25 cm class telescopes is sufficient to achieve near-complete coverage under nominal exclusion-zone constraints. Importantly, the simulations highlight that the limiting factor is often spatial coverage rather than sensitivity. The detectable population spans thousands of square degrees, requiring wide field of view sensors to efficiently tile the sky, which will in turn generate a large amount of imagery. In contrast, cislunar coverage is less sensitive to constellation size because exclusion zones and phase-angle geometry dominate observability. This suggests that cislunar SSA will require fundamentally different architectures, including sensors placed in or near the cislunar environment itself for full coverage. As cislunar pathfinder missions have begun over the past few years, opportunities to establish SSA methods from within the cislunar region should be explored.

Our binocular ranging experiments underscore the value of constellation geometry. With two satellites phased by 180°, position errors fell from several thousand kilometers to under 10 km, while velocity errors decreased from kilometers per second to meters per second. These gains directly impact initial orbit determination timelines and reduce the

Copyright © 2025 Advanced Maui Optical and Space Surveillance Technologies Conference (AMOS) – www.amostech.com

number of follow-up observations required. For operational networks, this indicates that constellation design should not only prioritize coverage but also baselines that maximize parallax.

6.2 Operational Considerations

A distributed COTS-based system offers multiple operational advantages. The use of edge computing reduces downlink volume by allowing onboard detection and compression of event-level data, mitigating one of the major bottlenecks in optical SSA. Autonomy also increases system resilience: individual satellites can operate semi-independently, while inter-satellite links allow detections to be cross-verified before downlink. From a deployment perspective, the modular architecture supports incremental growth, with new satellites added as budgets and launch opportunities permit. This approach lowers technical and financial barriers to entry, enabling not only national programs but also commercial and international collaborations.

However, operational limitations remain. The wide fields of view required for GEO coverage imply heavy background contamination, particularly in the galactic plane, which was not treated in this study. Furthermore, scheduling conflicts may arise when multiple high-priority targets fall within a single sensor's field. More detailed tasking simulations, including slewing, settling times, and pointing constraints, will be required to assess realistic cadence and duty cycles.

6.3 Limitations of the Present Study

Several simplifying assumptions should be noted. The photometric model assumed Lambertian reflectance and fixed albedo, whereas real spacecraft exhibit specular reflections, paneling, and strongly variable light curves. Detector models included only basic dark current and read noise; in practice, systematics such as hot pixels, radiation damage, and scattered light will affect performance. Similarly, the cislunar dynamics were modeled using circular restricted three-body problem [CR3BP 4, 7, 5, 9] seeds propagated over short timescales, whereas real cislunar trajectories are subject to perturbations from solar gravity, non-spherical Earth and lunar potentials, and stationkeeping maneuvers. While these assumptions suffice to capture first-order trends, higher-fidelity modeling will be required for mission design.

Finally, the constellation geometries considered here were limited to a single ring displaced from GEO. While this architecture is useful for parametric studies, it is unlikely to represent the optimal deployment for an operational system. More sophisticated optimization—balancing altitude, inclination, and longitude spacing—should be pursued to maximize both coverage and binocular parallax opportunities.

6.4 Future Directions

Future work should expand on three fronts. First, higher-fidelity modeling of optical signatures, incorporating both specular and diffuse scattering, would allow assessment of realistic detection completeness and false-alarm rates. Second, expanded orbit families should be considered for cislunar coverage, including near-rectilinear halo orbits [NRHO 15] and other dynamically stable regions of the Earth–Moon system. Third, optimization studies should identify constellation geometries that balance global coverage, binocular ranging opportunities, and launch cost. Ultimately, hardware validation through suborbital tests or hosted payloads will provide the most robust demonstration of COTS-based SSA concepts.

Our results support the conclusion that a distributed COTS constellation can form a scalable backbone for next-generation SSA. Such systems can reduce cost, increase resilience, and provide a practical pathway to extend awareness from GEO into the cislunar domain, supporting the long-term sustainability of human activity in space. The emergence of a robust small-satellite economy and ride-share programs should provide ample opportunities for demonstration missions in the coming years.

7. CONCLUSIONS

This study examined the feasibility of a distributed commercial off-the-shelf (COTS) satellite constellation for space situational awareness in GEO and cislunar regimes. Through simulations, we quantified how aperture size, constellation scale, and orbital geometry drive detection completeness and limiting magnitude. Results show that a modest constellation of 25 cm class telescopes placed in a GEO+1000 km ring can achieve high coverage of the GEO belt, while also offering partial visibility of representative cislunar trajectories. Importantly, we found that spatial coverage, rather than raw sensitivity, is the dominant challenge for GEO, whereas in cislunar space the primary limitation arises from exclusion zones and variable phase-angle geometry.

Copyright © 2025 Advanced Maui Optical and Space Surveillance Technologies Conference (AMOS) – www.amostech.com

Binocular ranging emerged as a particularly powerful tool. When two satellites are separated by 180° in longitude, position and velocity errors for cislunar targets decrease by several orders of magnitude compared to single-sensor fits. This indicates that constellation design should explicitly account for baselines that maximize parallax opportunities, as doing so can dramatically reduce the time and observations needed for accurate orbit determination.

Overall, our findings demonstrate that a scalable and cost-effective SSA architecture can be built on COTS technology. Such an approach complements traditional bespoke systems by offering rapid expandability, reduced cost per unit, and resilience through distribution. Although simplifying assumptions were made—particularly regarding target photometry, noise models, and orbit fidelity—the trends identified here provide a roadmap for future investigations. Continued refinement with higher-fidelity modeling, constellation optimization, and eventual hardware validation will be essential to transition these concepts from analysis to operational capability. Ultimately, distributed COTS constellations offer a practical path to extend SSA beyond GEO and in cislunar space itself.

8. REFERENCES

[1] Astropy Collaboration. Astropy: A community python package for astronomy. *AA*, 558:A33, 2013.

[2] Astropy Collaboration. The astropy project: Building an inclusive, open-science project. *AJ*, 156:123, 2018.

[3] Astropy Collaboration. The astropy project: Sustaining and growing a community-oriented open-source project. *ApJ*, 935:167, 2022.

[4] R. W. Farquhar. The control and use of libration-point satellites. Technical Report NASA TR R-346, NASA, 1969.

[5] G. Gómez, À. Jorba, J. Masdemont, and C. Simó. Dynamics and mission design near libration points: Volume iii—advanced methods. In *World Scientific Monograph Series in Mathematics*. World Scientific, 2001.

[6] R. H. Gooding. A new procedure for orbit determination from three angles. *Celest. Mech. Dyn. Astr.*, 57:237–261, 1993.

[7] Kathleen C. Howell. Three-dimensional, periodic, 'halo' orbits. *Celest. Mech.*, 32:53–71, 1984.

[8] T. Kelsall and et al. The cobe diffuse infrared background experiment search for the cosmic infrared background. ii. zodiacal light model and interplanetary dust cloud. *ApJ*, 508:44–73, 1998.

[9] W. S. Koon, M. W. Lo, J. E. Marsden, and S. D. Ross. *Dynamical Systems, the Three-Body Problem, and Space Mission Design*. Marsden Books, 2011.

[10] C. Leinert and et al. The 1997 reference of diffuse night sky brightness. *AAS*, 127:1–99, 1998.

[11] D. Mortari and M. Wilkins. Angles-only initial orbit determination: A linear algebraic solution. *J. Astronaut. Sci.*, 52:123–140, 2004.

[12] Alexander J. Pertica, Willem de Vries, Chris Shaffer, Jeremiah DiMatteo, Robert Goodloe, Emily Milne, Bailey Cortright, Weston Pruitt, Kyle Clarke, Brian Fox, Christian Fuller, and Michael Higgins. Sensitivity improvements for space domain awareness using satellite tracking on a nanosatellite. In *Proceedings of the Advanced Maui Optical and Space Surveillance Technologies Conference (AMOS)*, Maui, HI, 2023. Space-Based Assets track.

[13] B. D. Tapley, B. E. Schutz, and G. H. Born. *Statistical Orbit Determination*. Elsevier, 2004.

[14] Christopher N. A. Willmer. The absolute magnitude of the sun in several filters. *ApJS*, 236:47, 2018.

[15] Emily M. Zimovan, Kathleen C. Howell, and Diane C. Davis. Near rectilinear halo orbits and their application in cis-lunar space. In *3rd IAA Conference on Dynamics and Control of Space Systems (DyCoSS)*, RUDN University, Moscow, Russia, 2017. Paper IAA-AAS-DyCoSS3-125.

Copyright © 2025 Advanced Maui Optical and Space Surveillance Technologies Conference (AMOS) – www.amostech.com

9. ACKNOWLEDGMENTS

This work was performed under the auspices of the U.S. Department of Energy by Lawrence Livermore National Laboratory under Contract DE-AC52-07NA27344.

The LLNL document number is LLNL-CONF-2010753.

Copyright © 2025 Advanced Maui Optical and Space Surveillance Technologies Conference (AMOS) – www.amostech.com